

Dinuclear Cobalt(II) Complexes of an Acyclic Phenol-Based Dinucleating Ligand with Four Methoxyethyl Chelating Arms – First Magnetic Analyses in an Axially Distorted Octahedral Field

Hiroshi Sakiyama,^{*,[a]} Rie Ito,^[a] Hitoshi Kumagai,^[b] Katsuya Inoue,^[b]
Masatomi Sakamoto,^[a] Yuzo Nishida,^[a] and Mikio Yamasaki^[c]

Keywords: Dinuclear cobalt(II) complex / Dinucleating ligand / Crystal structure / Magnetic properties

An end-off type acyclic ligand with four methoxyethyl chelating arms, 2,6-bis[bis(2-methoxyethyl)aminomethyl]-4-methylphenol [H(bomp)], formed dinuclear cobalt(II) complexes [Co₂(bomp)(MeCO₂)₂]BPh₄ (**1**) and [Co₂(bomp)(PhCO₂)₂]BPh₄ (**2**). X-ray analysis revealed that complex **1**·CHCl₃ contains two cobalt ions bridged by a phenolic oxygen and two acetate groups, forming a μ -phenoxo-bis(μ -

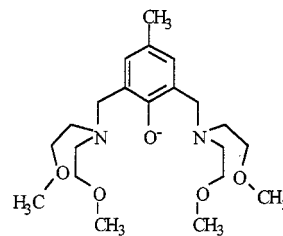
acetato)dicobalt(II) core. Magnetic susceptibility was measured for **1** and **2** over the temperature range 1.8–300 K. The data were successfully analyzed using a new theoretical method assuming an axially distorted octahedral field ($\Delta = 753$ and 775 cm⁻¹, respectively) for each cobalt(II) ion to reveal weak antiferromagnetic interactions ($J = -0.96$ and -1.74 cm⁻¹, respectively).

Introduction

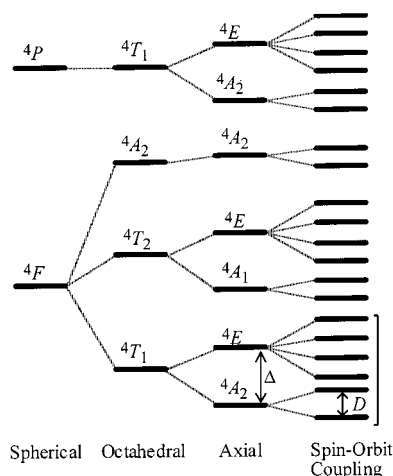
Dinuclear cobalt complexes have attracted our interest since the active site structure of methionine aminopeptidase (MAP, EC 3.4.11.18) was revealed to contain a bis(μ -carboxylato)dicobalt(II,II) core.^[1] From the point of view of coordination chemistry, it is interesting and invaluable to study the relationship between dinuclear structures and their properties and functions. In order to synthesize the dinuclear metal complexes systematically, the development of multinucleating ligands is of importance. We have developed an acyclic dinucleating ligand 2,6-bis[bis(2-methoxyethyl)aminomethyl]-4-methylphenol [H(bomp)].^[2] The dinuclear zinc(II) complexes^[2] and dinuclear manganese(II) complexes^[3] of this ligand have been reported. The ligand consists of a phenolate head unit, two aminomethyl shoulders, and four methoxyethyl arms, providing two NO₃ coordination sites. The dizinc(II) complexes have been shown to possess an aminopeptidase function in removing *N*-terminal amino acids from substrates, and the dimanganese(II) complexes have been demonstrated to have a catalytic catalase function in the disproportionation of hydrogen peroxide into water and molecular oxygen.

We are also interested in the magnetism of dinuclear cobalt(II,II) complexes. The lowest orbital state of the free cobalt(II) ion is 4F_1 , and the second lowest 4P_1 is more than

10⁴ cm⁻¹ higher. In the weak field of *O_h* symmetry,^[4] the 4F_1 term splits into $^4T_{1g}$, $^4T_{2g}$, and $^4A_{2g}$ terms, in that order, whereas the 4P_1 term is not split and remains in the $^4T_{1g}$ state. As the ground state of the high-spin cobalt(II) is $^4T_{1g}$,



Scheme 1



Scheme 2. Energy diagram for a high-spin cobalt(II) ion in an axially distorted octahedral environment

[a] Department of Material and Biological Chemistry, Faculty of Science, Yamagata University, Kojirakawa, Yamagata 990–8560, Japan
Fax: (internat.) +81–23–628–4591
E-mail: Saki@sci.kj.yamagata-u.ac.jp

[b] Institute for Molecular Science, Myodaiji, Okazaki 444–8585, Japan

[c] X-ray Research Laboratory, Rigaku Corporation, Matsubara 3-9-12, Akishima, Tokyo 196–8666, Japan

Supporting information for this article is available on the WWW under <http://www.wiley-vch.de/home/eurjic> or from the author.

under pure O_h symmetry, the contribution of the orbital momentum cannot be ignored, and it is the most significant one among 3d transition elements.^[5] The orbital momentum complicates the magnetic equations, a difficulty that has prevented many coordination chemists from analyzing the magnetic data of the cobalt(II) complexes.

As long ago as 1963, Lines introduced a calculation method for $^4T_{1g}$ -ground-state magnetism^[6] in an axially distorted octahedral field, considering the axial field splitting and the spin-orbit coupling. In the 1960s, Figgis also introduced a method considering the axial field for $^2T_{1g}$,^[7] $^3T_{1g}$,^[8] $^5T_{1g}$,^[9] and $^4T_{1g}$,^[10] showing that the axial field treatment is useful for analyzing cryomagnetic data of mononuclear cobalt(II) complexes. This successful study corresponded to a mononuclear case, but, in 1971, Lines reported a theory for the analysis of the magnetic coupling between two high-spin cobalt(II) ions of pure O_h symmetry using temperature-dependent Hamiltonian.^[11] This remarkable theory enabled the analysis of the magnetic data of some dinuclear cobalt(II) complexes,^[12] but it was limited to only highly symmetrical cases.

In this study, we have synthesized new dicobalt(II) complexes using the dinucleating ligand bomp^- , and their cryomagnetic data have been analyzed using a newly obtained set of magnetic equations for dinuclear cobalt(II) complexes in lower symmetry. In this method, the axial splitting parameter Δ is adopted according to Figgis and Lines, avoiding overparameterization, to describe the axial distortion. The axial splitting parameter Δ is defined as the splitting of the orbital degeneracy of the $^4T_{1g}$ term by the asymmetric ligand component, in the absence of any spin-orbit coupling, and is taken to be positive when the orbital singlet is lowest. This enables us to analyze the data using only four variables, the axial splitting parameter Δ , the spin-orbit coupling λ , the orbital reduction factor κ , and the coupling constant J . The axial zero-field splitting parameter D and the anisotropic g -factors, g_z and g_x , can be calculated using the four variables. To the best of our knowledge, this is the first standard analytic method for the magnetism of dinuclear high-spin cobalt(II) complexes in lower symmetry, except for the specific low-temperature study,^[13] and these complexes are the first examples whose cryomagnetic data are analyzed in the whole temperature range using the method in lower symmetry.

Results and Discussion

X-ray Crystal Structure of Complex $1 \cdot \text{CHCl}_3$

The crystal structure consists of $[\text{Co}_2(\text{bomp})(\text{MeCO}_2)_2]^+$ complex cations, tetraphenylborate anions, and chloroform molecules in a 1:1:1 molar ratio. The structure of the complex cation is depicted in Figure 1. Selected distances and angles with their estimated standard deviations are listed in Tables 1 and 2. The complex cation consists of one dinucleating ligand bomp^- , two cobalt(II) ions, and two acetate groups. The two cobalt ions are bridged by the one phenolic

oxygen of bomp^- and the two acetate ions, forming a μ -phenoxo-bis(μ -acetato)dicobalt(II) core structure. The $\text{Co}(1) \cdots \text{Co}(2)$ separation is 3.3360(3) Å.

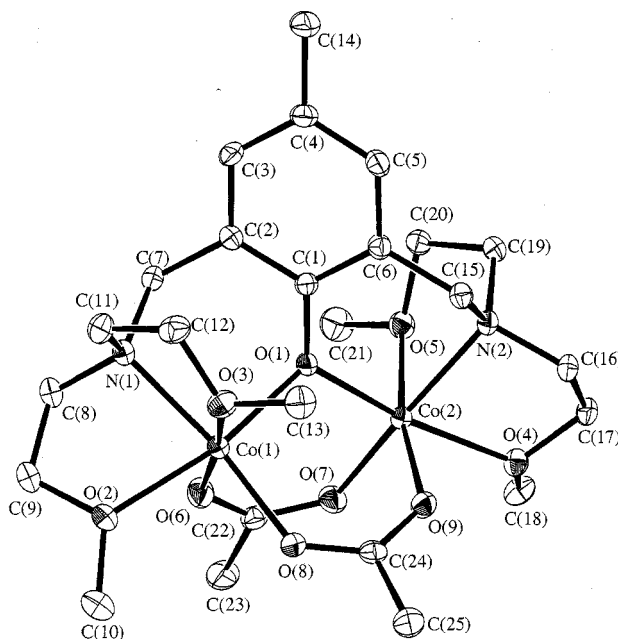


Figure 1. ORTEP^[14] view of complex cation $[\text{Co}_2(\text{bomp})(\text{MeCO}_2)_2]^+$ with the atom numbering scheme

Table 1. Selected distances (Å) for complex $1 \cdot \text{CHCl}_3$

atom	atom	distance	atom	atom	distance
Co(1)	O(1)	1.995(1)	Co(2)	O(1)	2.005(1)
Co(1)	O(2)	2.160(1)	Co(2)	O(4)	2.156(1)
Co(1)	O(3)	2.200(1)	Co(2)	O(5)	2.229(1)
Co(1)	O(6)	2.069(2)	Co(2)	O(7)	2.028(2)
Co(1)	O(8)	2.027(1)	Co(2)	O(9)	2.084(1)
Co(1)	N(1)	2.141(2)	Co(2)	N(2)	2.144(2)
Co(1)	Co(2)	3.3360(3)			

Table 2. Selected angles (°) for complex $1 \cdot \text{CHCl}_3$

atom	atom	atom	angle	atom	atom	atom	angle
O(1)	Co(1)	O(2)	166.04(6)	O(1)	Co(2)	O(4)	170.53(5)
O(1)	Co(1)	O(3)	93.73(6)	O(1)	Co(2)	O(5)	95.77(5)
O(1)	Co(1)	O(6)	92.46(6)	O(1)	Co(2)	O(7)	99.00(6)
O(1)	Co(1)	O(8)	100.27(6)	O(1)	Co(2)	O(9)	92.57(5)
O(1)	Co(1)	N(1)	92.07(6)	O(1)	Co(2)	N(2)	90.81(6)
O(2)	Co(1)	O(3)	91.23(6)	O(4)	Co(2)	O(5)	84.68(5)
O(2)	Co(1)	O(6)	82.16(6)	O(4)	Co(2)	O(7)	90.45(5)
O(2)	Co(1)	O(8)	92.90(6)	O(4)	Co(2)	O(9)	86.17(5)
O(2)	Co(1)	N(1)	76.20(6)	O(4)	Co(2)	N(2)	80.06(6)
O(3)	Co(1)	O(6)	173.29(6)	O(5)	Co(2)	O(7)	89.99(6)
O(3)	Co(1)	O(8)	88.47(6)	O(5)	Co(2)	O(9)	169.92(5)
O(3)	Co(1)	N(1)	78.02(6)	O(5)	Co(2)	N(2)	77.12(6)
O(6)	Co(1)	O(8)	92.98(6)	O(7)	Co(2)	O(9)	94.30(6)
O(6)	Co(1)	N(1)	99.17(6)	O(7)	Co(2)	N(2)	164.57(6)
O(8)	Co(1)	N(1)	162.30(6)	O(9)	Co(2)	N(2)	97.15(6)

Co(1) has a distorted octahedral geometry with O(1), O(2), O(3), and N(1) of *bomp*[−] and O(6) and O(8) of the two acetate groups. Coordination geometry around Co(2) is also distorted octahedral with O(1), O(4), O(5), and N(2) of *bomp*[−] and O(7) and O(9) of the two acetate groups. The geometries around Co(1) and Co(2) are very similar to each other, and the complex cation has a pseudo *C*₂ axis along C(14), C(4), C(1), and O(1). The least-squares plane of the aromatic ring of *bomp*[−] and the plane defined by Co(1), Co(2), and O(1) are twisted with a dihedral angle of 46.0°. The bond lengths between the cobalt atoms and axial ether oxygen atoms [2.200(1)–2.229(1) Å] are longer than those between cobalt atoms and equatorial ether oxygen atoms [2.156(1)–2.160(1) Å] (Figure 2). This tendency has also been observed in the related dizinc(II) complexes with acetate bridges.^[2] However, in the dimanganese(II) complexes with benzoate bridges, all the manganese-oxygen(ether) bonds have almost the same length.^[3] This may be explained by the steric repulsion between the two bridging benzoate ions and methoxy groups of the dinucleating ligand *bomp*[−]. Thus, the symmetry around the metal ions in the benzoate-bridged complex cations is higher than that of the acetate complexes.

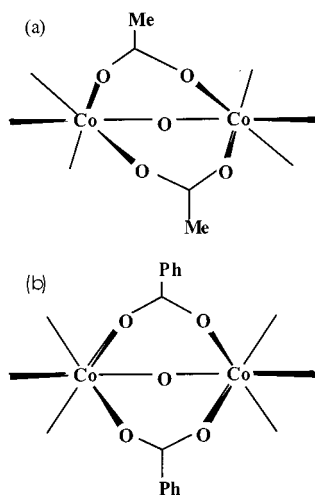


Figure 2. Schematic drawing of dinuclear cobalt(II) cores for (a) complex **1** and (b) complex **2**

Magnetic Susceptibility of Complexes **1** and **2**

Magnetic susceptibility measurements for cobalt complexes **1** and **2** were made on polycrystalline samples in the temperature range 1.8–300 K. The temperature dependence of χ_A and μ_{eff} per Co for **1** and **2** is shown in Figures 3 and 4. The μ_{eff} values per Co^{II} of the complexes at room temperature are 4.93 and 4.90 μ_B , respectively. These values are larger than the spin-only value of high-spin cobalt(II) (3.87 μ_B ; $\mu_{SO} = [4S(S + 1)]^{1/2}$; $S = 3/2$), but close to the value expected when the spin momentum and the orbital momentum exist independently [5.20 μ_B ; $\mu_{LS} = [L(L + 1) + 4S(S + 1)]^{1/2}$; $L = 3$, $S = 3/2$]. This indicates a contribution of the orbital momentum typical for the ⁴T_{1g} ground

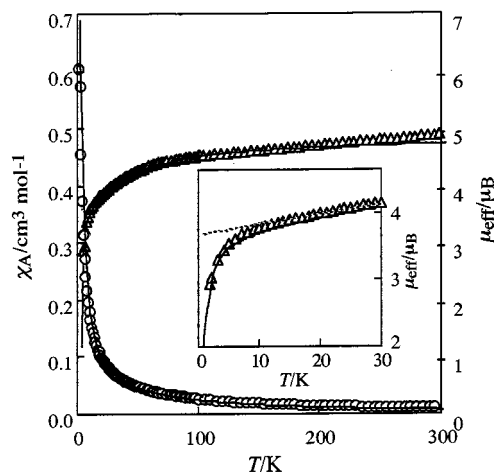


Figure 3. Temperature dependence of χ_A (O) and μ_{eff} (Δ) of the complex **1**. Dashed curves are based on equations (2a) in the text, using $\kappa = 0.96$, $\lambda = -140 \text{ cm}^{-1}$, and $\Delta = 753 \text{ cm}^{-1}$. Solid curves are based on a set of equations in the supplementary material section, using $\kappa = 0.96$, $\lambda = -140 \text{ cm}^{-1}$, $\Delta = 753 \text{ cm}^{-1}$, and $J = -0.96 \text{ cm}^{-1}$.

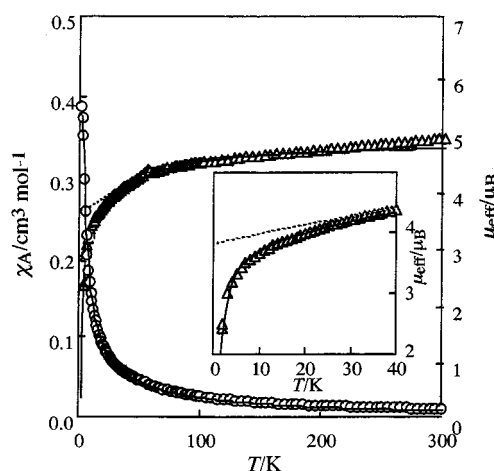


Figure 4. Temperature dependence of χ_A (O) and μ_{eff} (Δ) of the complex **2**. Dashed curves are based on equations (2a) in the text, using $\kappa = 0.92$, $\lambda = -156 \text{ cm}^{-1}$, and $\Delta = 775 \text{ cm}^{-1}$. Solid curves are based on a set of equations in the supplementary material section, using $\kappa = 0.92$, $\lambda = -156 \text{ cm}^{-1}$, $\Delta = 775 \text{ cm}^{-1}$, and $J = -1.74 \text{ cm}^{-1}$.

state. The magnetic moments decrease with decreasing temperature, and three factors are considered to elucidate this phenomenon; (1) the contribution of the orbital momentum, (2) an intramolecular antiferromagnetic coupling between two Co^{II} centers, and (3) an intermolecular antiferromagnetic coupling. However, we neglect the intermolecular coupling in this study since the X-ray analysis shows the dinuclear cobalt(II) centers to be well separated from each other. In order to evaluate the two remaining effects, we first tried to analyze the experimental cryomagnetic data using the isotropic one-ion approximation with the spin-orbit coupling in pure *O_h* symmetry, $H = -(3/2)\kappa \lambda L \cdot S + \beta[-(3/2)\kappa L + g_e S] \cdot H$. A magnetic susceptibility equation was obtained as follows;^[5,10]

$$\chi_A = \frac{N\beta^2}{kT} \frac{F_1}{F_2} \quad (1a)$$

$$F_1 = \frac{63}{20}(-2 + \kappa)^2 x + \frac{2(4 + 3\kappa)^2}{25\kappa} + \left[\frac{2}{45}(11 - 3\kappa)^2 x + \frac{88(4 + 3\kappa)^2}{2025\kappa} \right] \exp\left(-\frac{15\kappa}{4}x\right) + \left[\frac{1}{36}(10 + 3\kappa)^2 x - \frac{10(4 + 3\kappa)^2}{81\kappa} \right] \exp(-6\kappa x) \quad (1b)$$

$$F_2 = x[3 + 2 \exp(-\frac{15\kappa}{4}x) + \exp(-6\kappa x)] \quad (1c)$$

where $x = \lambda/(kT)$, λ is the spin-orbit coupling, κ is the orbital reduction factor, and other symbols have their usual meanings. The cryomagnetic data could not be explained by this equation. The magnetic interaction between intramolecular two cobalt(II) ions has also been taken into consideration using Lines' isotropic theory,^[11] but the simulation was not successful. This is probably due to the trigonal distortion around the cobalt(II) centers.

Secondly, we considered the distortion around the cobalt(II) ions for the magnetic data analysis introducing the axial splitting parameter Δ . It has been shown that the axial parameter Δ can be used in both the trigonal and the tetragonal field.^[7,8] In the higher temperature range ($kT \gg |J|$), one-ion approximation is available, and a magnetic susceptibility equation for a mononuclear model was obtained^[5,6,10] using the van Vleck formula^[15] as follows;

$$\chi_A = \frac{\chi_z + 2\chi_x}{3} \quad (2a)$$

$$\chi_{z(x)} = N \frac{\sum_n \left(\frac{E_n^{(1)}}{kT} \right)^2 - 2 \frac{E_{n,z(x)}^{(2)}}{kT} \exp\left[-\frac{E_n^{(0)}}{kT}\right]}{\sum_n \exp\left[-\frac{E_n^{(0)}}{kT}\right]} \quad (2b)$$

Energies $E_n^{(0)}$, $E_{n,z(x)}^{(1)}$, and $E_{n,z(x)}^{(2)}$ ($n = \pm 1 - \pm 6$) were calculated by solving the 12×12 secular matrix,^[5,6] and the resulting energy equations are shown in the supplementary material section. An important feature of this method is that only three parameters, namely, κ , λ , and Δ , are required for analyzing the cryomagnetic data in an axially distorted octahedral field. The data were well simulated in the temperature range 50–300 K for each complex, and calculated curves are also shown in Figure 3 and 4. Fitting parameters were $\kappa = 0.96$, $\lambda = -140 \text{ cm}^{-1}$, and $\Delta = 753 \text{ cm}^{-1}$ for complex **1**, and $\kappa = 0.92$, $\lambda = -156 \text{ cm}^{-1}$, and $\Delta = 775 \text{ cm}^{-1}$ for **2**. The g values were calculated as $g_z = 2.18$ and $g_x = 4.97$ for **1** and $g_z = 2.20$ and $g_x = 4.93$ for **2**. Agreement factors defined as $R = \sum(\chi_A^{\text{calcd.}} - \chi_A^{\text{obs}})^2 / \sum(\chi_A^{\text{obs}})^2$ were 1.4×10^{-4} and 3.6×10^{-4} , respectively.

The spin-orbit coupling λ for cobalt(II) ion is theoretically expected to be -172 cm^{-1} . The λ value for the complex **2** is slightly smaller than this, and the value for complex **1** is much smaller. The orbital reduction factor κ means the reduction of the orbital momentum caused by the delocalization of the unpaired electrons, but it also contains the admixture of the upper $^4T_{1g}(^4P_1)$ state into the $^4T_{1g}(^4F_1)$

ground state. In the free cobalt(II) ion, $\kappa_{\text{free ion}}$ is known to be ≈ 0.93 ,^[11,16] but smaller values such as ≈ 0.75 are also obtained when the physical distortion is large.^[11] Known values of the axial splitting Δ are in the range $\approx 200 - \approx 800 \text{ cm}^{-1}$.^[10] The three parameters obtained for complex **2** are normal, while the parameters for **1** deviate slightly from the normal values. This can be explained by the fact that the symmetry of complex **1** is lower than that of **2**. Thus, the axial approximation is adequate for **2**, but not so much for **1**. In any case, in the low-temperature range, the observed data for both complexes were smaller than the calculated values in one-ion approximation, indicating antiferromagnetic interaction between two cobalt(II) ions in the complex cation.

Finally, the interaction between two cobalt(II) ions is introduced to the axial mononuclear model as a perturbation; $H = -(3/2)\kappa \lambda \mathbf{L} \cdot \mathbf{S} + \beta[-(3/2)\kappa \mathbf{L} + g_e \mathbf{S}] \cdot \mathbf{H} - J \mathbf{S}_1 \cdot \mathbf{S}_2$. When Δ values are in the range $700 - 800 \text{ cm}^{-1}$, the energy separation between the lowest and the second lowest Kramers doublets, which corresponds to the axial zero-field splitting D , is estimated to be $120 - 200 \text{ cm}^{-1}$. The magnitude of the coupling constant J is expected to be smaller than 2 cm^{-1} ($|J| < 2 \text{ cm}^{-1}$) since the susceptibility maximum was not observed^[5] in either complex. In these cases ($|J| \ll |D|$), the perturbation of the magnetic coupling is effective only in the lowest doublet. In other words, upper states can be ignored when the magnetic interaction is observed in the lower-temperature range ($|J| \approx kT \ll |D|$), while the magnetic interaction can be neglected when the second lowest state is thermally populated in the higher-temperature range ($|J| \ll |D| \approx kT$). The same one-ion energy equations can be used, but the susceptibility equations were slightly modified (see supplementary material section). The data were well simulated in the whole temperature range using four parameters, namely, κ , λ , Δ , and J . The best-fitting parameters were $\kappa = 0.96$, $\lambda = -140 \text{ cm}^{-1}$, $\Delta = 753 \text{ cm}^{-1}$, $J = -0.96 \text{ cm}^{-1}$, $g_z = 2.18$, and $g_x = 4.97$, and $R = 5.3 \times 10^{-4}$ for complex **1**. The corresponding parameters for complex **2** were $\kappa = 0.92$, $\lambda = -156 \text{ cm}^{-1}$, $\Delta = 775 \text{ cm}^{-1}$, $J = -1.74 \text{ cm}^{-1}$, $g_z = 2.20$, $g_x = 4.93$, and $R = 3.6 \times 10^{-4}$ (Table 3). In order to ascertain the resulting parameters, the low-temperature data ($T < 30$) were also analyzed by the method considering only the ground Kramers doublet,^[13] using the g -factors obtained above. The results were $J = -0.85 \text{ cm}^{-1}$, $g_z = 2.18$, $g_x = 4.97$, $N\mu = 0.35 \text{ cm}^3 \text{ mol}^{-1}$, $R = 7.5 \times 10^{-5}$ for **1** and $J = -1.54 \text{ cm}^{-1}$, $g_z = 2.20$, $g_x = 4.93$, $N\mu = 0.24 \text{ cm}^3 \text{ mol}^{-1}$, $R = 3.9 \times 10^{-4}$ for **2**. The J value obtained previously for each complex is in good agreement with the corresponding value obtained from the low-temperature data.

Table 3. Magnetic data for complexes **1** and **2**

Complex	κ	λ/cm^{-1}	Δ/cm^{-1}	J/cm^{-1}	g_z	g_x	D/cm^{-1}	$R/10^{-4}$
1	0.96	-140	753	-0.96	2.18	4.97	125	5.3
2	0.92	-156	775	-1.74	2.20	4.93	138	3.6

Limitations of Our New Theoretical Method

In this study, we have developed a new equation set for analyzing the magnetism of dinuclear high-spin cobalt(II) complexes in lower symmetry. Axial symmetry has been assumed for each cobalt(II) ion; thus, the theory is available for a trigonally-distorted octahedral field and a tetragonally-distorted one. When the symmetry around the cobalt(II) ions is rhombic and cannot be approximated by the axial field, this method is no longer useful. When the magnetic coupling between any cobalt(II) ions is negligible ($J = 0$), the magnetic equation set is completely the same as that of the axially distorted mononuclear model of Figgis and Lines. In the present theory, magnetic coupling was considered only for the lowest doublet. This approximation is valid when the coupling constant J is much smaller than the axial zero-field splitting D ($|J| \ll |D|$). It has been reported that the axial splitting Δ of the cobalt(II) ions in normal mononuclear cobalt(II) complexes is in the range 200–800 cm^{-1} ,^[10] and the axial zero-field splitting is in the range 120–330 cm^{-1} . Usually, the magnitude of the coupling constant J is smaller than 10 cm^{-1} ($|J| < 10 \text{ cm}^{-1}$); thus, the approximation we used in this study is expected to be useful for most dinuclear high-spin cobalt(II) complexes. However, it should be emphasized again that there is a limit in the symmetry around the cobalt(II) ion. (1) If the symmetry is isotropic ($\Delta \approx 0$), Lines' theory^[11] would be preferable for the estimation of the J value. (2) If the symmetry is axial, the method we have shown in this study may be more useful than Lines' theory. (3) If the symmetry is rhombic, no method is useful at this moment, to the best of our knowledge.

Conclusion

In this study, two dinuclear cobalt(II) complexes (**1** and **2**) were made using the dinucleating ligand, bomp^- , and the crystal structure of complex **1** was determined. For the purpose of analyzing the cryomagnetic data, a new theoretical method was developed assuming an axially distorted octahedral field, and the experimental data were analyzed. This is the first successful magnetic analysis for dinuclear high-spin cobalt(II) complexes in an axially distorted octahedral field.

Experimental Section

Measurements: Elemental analyses were obtained at the Elemental Analysis Service Centre of Kyushu University. – Infrared (IR) spectra were recorded on a Hitachi 270–50 spectrophotometer. – Fast atom bombardment (FAB) mass spectra were measured on a Fisons ZabSpec Q mass spectrometer in *N,N*-dimethylformamide (DMF) with a glycerol matrix. – Molar conductances were measured on a DKK AOL-10 conductivity meter at room temperature. – Electronic spectra were recorded on a Shimadzu UV-240 spectrophotometer. – Magnetic susceptibility was measured between 1.8 and 300 K by using a Quantum Design SQUID magnetometer

MPMS-5S in fields up to 5 T. All the magnetic calculations were made using the MagSaki^[17] magnetic software program of our laboratory.

Materials: All chemicals were commercial products, and were used as supplied. The ligand Na(bomp) was prepared by the method reported previously.^[2]

Synthesis of $[\text{Co}_2(\text{bomp})(\text{MeCO}_2)_2]\text{BPh}_4$ (1**):** To a methanolic solution (15 mL) of Na(bomp) (1.0 mmol, 0.42 g) was added cobalt(II) acetate dihydrate (2.0 mmol, 0.50 g), and the resulting solution was heated under reflux for 1 h to give a pink solution. The addition of sodium tetraphenylborate (1.0 mmol, 0.34 g) resulted in the precipitation of pink microcrystals. The compound was recrystallized from a mixture of acetonitrile and 2-propanol. Yield: 0.23 g (24%). – $\text{C}_{49}\text{H}_{63}\text{BCo}_2\text{N}_2\text{O}_9$: calcd. C 61.75, H 6.65, N 2.95, Co 12.4; found C 61.60, H 6.65, N 2.90, Co 12.4. – Selected IR data (KBr): $\tilde{\nu} = 3050\text{--}2900, 1600, 1410, 1090, 730, 700 \text{ cm}^{-1}$. – FAB mass spectrum: $m/z = 633 [\text{Co}_2(\text{bomp})(\text{MeCO}_2)_2]^+$. – Molar conductance [in DMF] = 46 $\text{A}_\text{M}/\text{Scm}^2\text{mol}^{-1}$. – UV/Vis: λ_{max} ($\epsilon/\text{dm}^3\text{cm}^{-1}\text{mol}^{-1}$, in DMF) = 485 (30), 512 (35) nm.

Synthesis of $[\text{Co}_2(\text{bomp})(\text{PhCO}_2)_2]\text{BPh}_4$ (2**):** This was prepared as pink microcrystals by a method similar to that of **1**, using cobalt(II) benzoate instead of cobalt(II) acetate tetrahydrate. Yield: 0.24 g (23%). – $\text{C}_{59}\text{H}_{67}\text{BCo}_2\text{N}_2\text{O}_9$: calcd. C 65.80, H 6.25, N 2.60, Co 11.0; found C 65.80, H 6.25, N 2.60, Co 10.9. – Selected IR data (KBr): $\tilde{\nu} = 3050\text{--}2900, 1610, 1400, 1085, 730, 700 \text{ cm}^{-1}$. – FAB mass spectrum: $m/z = 757 [\text{Co}_2(\text{bomp})(\text{PhCO}_2)_2]^+$. – Molar conductance (in DMF) = 43 $\text{A}_\text{M}/\text{Scm}^2\text{mol}^{-1}$. – UV/Vis λ_{max} ($\epsilon/\text{dm}^3\text{cm}^{-1}\text{mol}^{-1}$, in DMF) = 480 (40), 510 (45) nm.

Single Crystal X-ray Analysis of Complex **1·CHCl₃:** Crystal data: $\text{C}_{50}\text{H}_{64}\text{BCo}_2\text{Cl}_3\text{N}_2\text{O}_9$, $M = 1072.10$, $a = 13.2229(6)$, $b = 14.5043(9)$, $c = 16.0204(8) \text{ Å}$, $\alpha = 68.8982(6)$, $\beta = 82.022(1)$, $\gamma = 64.279(2)^\circ$, $V = 2581.9(2) \text{ Å}^3$, $Z = 2$, $d_{\text{calcd.}} = 1.379 \text{ g cm}^{-3}$, triclinic, space group $P\bar{1}$ (no. 2), $F(000) = 1120.00$. Data collection: A purple prismatic crystal of **1**·CHCl₃ having approximate dimensions of $0.40 \times 0.40 \times 0.30 \text{ mm}$ was mounted in a loop. All measurements were made on Rigaku/MSC Mercury CCD diffractometer with graphite monochromated Mo- K_α radiation ($\lambda = 0.71069 \text{ Å}$). The ω scan was made to a maximum 2θ value of 54.6° at $-170 \pm 1^\circ \text{C}$. Of the 29279 reflections, 11541 were unique ($R_{\text{int}} = 0.019$), and $I > 2.0 \sigma(I)$ data were used. The linear absorption coefficient $\mu(\text{Mo-}K_\alpha)$ was 8.53 cm^{-1} . A symmetry-related absorption correction was applied, which resulted in transmission factors ranging from 0.62 to 0.77. The data were corrected for Lorentz and polarization effects. – Structural analysis and refinement: The structure was solved by direct methods,^[18] and expanded using Fourier techniques.^[19] The non-hydrogen atoms were refined anisotropically. Hydrogen atoms were refined isotropically. The final cycle of full-matrix least-squares refinement was based on 11541 observed reflections. The final values of R and R_w were 0.065 and 0.147, respectively ($R = \Sigma||F_o| - |F_c||/\Sigma |F_o|$, $R_w = \{\Sigma w(|F_o| - |F_c|)^2/\Sigma wF_o^2\}^{1/2}$). All calculations were performed using the teXsan^[20] crystallographic software package of Molecular Structure Corporation.

Crystallographic data (excluding structure factors) for the structure(s) included in this paper have been deposited with the Cambridge Crystallographic Data Centre as supplementary publication no. CCDC-151304. Copies of the data can be obtained free of charge on application to CCDC, 12 Union Road, Cambridge CB2 1EZ, UK [Fax: (internat.) +44-1223/336-033; E-mail: deposit@ccdc.cam.ac.uk].

Acknowledgments

The author thanks Professor Hisashi Okawa for his encouragement.

- [1] S. L. Roderick, B. W. Matthews, *Biochemistry* **1993**, *32*, 3907–3912.
- [2] H. Sakiyama, R. Mochizuki, A. Sugawara, M. Sakamoto, Y. Nishida, M. Yamasaki, *J. Chem. Soc., Dalton Trans.* **1999**, 997–1000.
- [3] H. Sakiyama, A. Sugawara, M. Sakamoto, Y. Nishida, K. Inoue, M. Yamasaki, *Inorg. Chim. Acta* **2000**, *310*, 163–168.
- [4] B. N. Figgis, M. A. Hitchman, *Ligand Field Theory and its Applications*, Wiley-VCH, **2000**.
- [5] O. Kahn, *Molecular Magnetism*, VCH, **1993**.
- [6] M. E. Lines, *Phys. Rev.* **1963**, 546–555.
- [7] B. N. Figgis, *Trans. Faraday Soc.* **1961**, *57*, 198–203.
- [8] B. N. Figgis, J. Lewis, F. E. Mabbs, G. A. Webb, *J. Chem. Soc. A* **1966**, 1411–1421.
- [9] B. N. Figgis, J. Lewis, F. E. Mabbs, G. A. Webb, *J. Chem. Soc. A* **1967**, 442–447.
- [10] B. N. Figgis, M. Gerloch, J. Lewis, F. E. Mabbs, G. A. Webb, *J. Chem. Soc. A* **1968**, 2086–2093.
- [11] M. E. Lines, *J. Chem. Phys.* **1971**, *55*, 2977–2984.
- [12] G. D. Munno, M. Julve, F. Lloret, J. Faus, A. Caneschi, *J. Chem. Soc., Dalton Trans.* **1994**, 1175–1183.
- [13] E. Coronado, M. Drillon, P. R. Nugteren, L. J. de Jongh, D. Beltran, *J. Am. Chem. Soc.* **1988**, *110*, 3907–3913.
- [14] C. K. Johnson, *ORTEP*, Oak Ridge National Laboratory, **1976**.
- [15] J. H. Van Vleck, *The Theory of Electronic and Magnetic Susceptibilities*, Oxford University Press, Oxford, **1932**.
- [16] W. Low, *Phys. Rev.* **1958**, *109*, 256–265.
- [17] H. Sakiyama, *MagSaki*, Sakiyama Laboratory, **2000**.
- [18] A. Altomare, M. C. Burla, M. Camalli, G. L. Cascarano, C. Giacovazzo, A. Guagliardi, A. G. G. Moliterni, G. Polidori, R. Spagna, *J. Appl. Cryst.* **1999**, *32*, 115–119.
- [19] P. T. Beurskens, G. Admiraal, G. Beurskens, W. P. Bosman, R. de Gelder, R. Israel, J. M. M. Smits, *DIRDIF-94*, University of Nijmegen, **1994**.
- [20] Crystal Structure Analysis Package, Molecular Structure Corporation, **1985, 1999**.

Received November 6, 2000
[100420]